# *Conserved hippocampal cellular pathophysiology but distinct behavioural deficits in a new rat model of FXS*



**Citation:** Till, Sally M., Antonis Asiminas, Adam D. Jackson, Danai Katsanevaki, Stephanie A. Barnes, Emily K. Osterweil, Mark F. Bear, et al. "Conserved Hippocampal Cellular Pathophysiology but Distinct Behavioural Deficits in a New Rat Model of FXS." Human Molecular Genetics 24, no. 21 (August 4, 2015): 5977–5984.

**As Published:** http://dx.doi.org/10.1093/hmg/ddv299

**Publisher:** Oxford University Press

**Persistent URL:** http://hdl.handle.net/1721.1/102350

**Version:** Final published version: final published article, as it appeared in a journal, conference proceedings, or other formally published context

*Human Molecular Genetics*, 2015, Vol. 24, No. 21 5977–5984

**doi: 10.1093/hmg/ddv299**
Advance Access Publication Date: 4 August 2015
Original Article

ORIGINAL ARTICLE

# Conserved hippocampal cellular pathophysiology but distinct behavioural deficits in a new rat model of FXS

Sally M. Till[1,2,†], Antonis Asiminas[1,3], Adam D. Jackson[2,4,‡], Danai Katsanevaki[1,2,‡], Stephanie A. Barnes[1,2], Emily K. Osterweil[1,2,5], Mark F. Bear[5], Sumantra Chattarji[1,4,6], Emma R. Wood[1,3,†], David J.A. Wyllie[1,2,4,†] and Peter C. Kind[1,2,4,†,*]

[1]Patrick Wild Centre, [2]Centre for Integrative Physiology, The University of Edinburgh, Edinburgh EH8 9XD, UK, [3]Centre for Cognitive and Neural Systems, The University of Edinburgh, Edinburgh EH8 9JZ, UK, [4]Centre for Brain Development and Repair, The Institute for Stem Cell Biology and Regenerative Medicine, Bangalore 560065, India, [5]Department of Brain and Cognitive Sciences, Howard Hughes Medical Institute, Picower Institute for Learning and Memory, Massachusetts Institute of Technology, Cambridge MA 02139, USA and [6]National Centre for Biological Sciences, Tata Institute of Fundamental Research, Bangalore 560065, India

*To whom correspondence should be addressed at: University of Edinburgh, Hugh Robson Building George Square, EH8 9XD, UK. Tel: +0131 6511762; Fax: +0131 6511706; Email: pkind@ed.ac.uk

## Abstract

Recent advances in techniques for manipulating genomes have allowed the generation of transgenic animals other than mice. These new models enable cross-mammalian comparison of neurological disease from core cellular pathophysiology to circuit and behavioural endophenotypes. Moreover they will enable us to directly test whether common cellular dysfunction or behavioural outcomes of a genetic mutation are more conserved across species. Using a new rat model of Fragile X Syndrome, we report that *Fmr1* knockout (KO) rats exhibit elevated basal protein synthesis and an increase in mGluR-dependent long-term depression in CA1 of the hippocampus that is independent of new protein synthesis. These defects in plasticity are accompanied by an increase in dendritic spine density selectively in apical dendrites and subtle changes in dendritic spine morphology of CA1 pyramidal neurons. Behaviourally, *Fmr1* KO rats show deficits in hippocampal-dependent, but not hippocampal-independent, forms of associative recognition memory indicating that the loss of fragile X mental retardation protein (FMRP) causes defects in episodic-like memory. In contrast to previous reports from mice, *Fmr1* KO rats show no deficits in spatial reference memory reversal learning. One-trial spatial learning in a delayed matching to place water maze task was also not affected by the loss of FMRP in rats. This is the first evidence for conservation across mammalian species of cellular and physiological hippocampal phenotypes associated with the loss of FMRP. Furthermore, while key cellular phenotypes are conserved they manifest in distinct behavioural dysfunction. Finally, our data reveal novel information about the selective role of FMRP in hippocampus-dependent associative memory.

†To whom correspondence can be addressed.
‡ADJ and DK contributed equally to this study and are listed in alphabetical order.
**Received:** June 17, 2015. **Revised and Accepted:** July 21, 2015

## Introduction

Although mice and other model organisms have been, and continue to be valuable models of neurodevelopmental disorders (NDDs), the development of genetically engineered rats allows for extended modelling of several key aspects of these disorders including complex cognitive and social functions and non-invasive imaging. Furthermore, rats and mice separated in evolution over 12 million years ago, and comparison across these mammalian species will be essential for determining whether conserved cellular phenotypes result in similar circuit and/or behavioural outcomes. While rat models can have a significant impact on our understanding of neurological disease, experimental interpretation will be prone to the untested assumption that cellular phenotypes between mouse and rat models are conserved. Therefore an essential first step to realizing the potential of rat models of NDDs is to directly compare key phenotypes associated with analogous mutations in mice or other species.

Fragile X Syndrome (FXS), the most common form of inherited intellectual disability, is caused by mutations in the *FMR1* gene that lead to loss of the protein it encodes, fragile X mental retardation protein (FMRP). Notable hippocampal phenotypes in *Fmr1* knockout (KO) mice include enhanced expression of group 1 metabotropic glutamate-receptor mediated long-term depression (mGluR-LTD) in the hippocampus (1) and protein synthesis-independent maintenance of this form of persistent plasticity (2). In agreement with the known role for FMRP in regulating protein synthesis (3), *Fmr1* KO mice show elevated levels of basal protein synthesis (4–6). These functional changes are accompanied by alterations in dendritic spine structure (7). While loss of FMRP does not affect performance in a hippocampus-dependent reference memory version of the Morris water maze, *Fmr1* KO mice are impaired in reversal learning (8–11).

Using a rat model of FXS we demonstrate that several key cellular deficits in hippocampus that result from *Fmr1* deletion are conserved between species that separated in evolution more than 12 million years ago (12). Building on this comparison of cellular phenotypes between the two species, we further report deficits in hippocampal-dependent, but not hippocampal-independent, novelty based exploration tasks. Importantly, unlike in the mouse, performance in spatial reference memory, reversal learning and delayed matching to place (DMP) tasks were not altered in *Fmr1* KO rats, indicating rat-specific hippocampal-based memory behaviours in the absence of FMRP. In summary, rats show species-specific behavioural deficits in the absence of FMRP despite conservation of cellular deficits.

## Results

### Dynamic FMRP expression in brain during postnatal development

To determine whether the spatiotemporal expression of FMRP in rats is similar to that described in mice (13), coronal slices were prepared from wild-type (WT) Sprague Dawley (SD) rats at various developmental ages and immunolabelled for FMRP. We found that FMRP is widely expressed throughout the brain, including the hippocampus and neocortex during the first few weeks after birth (Fig. 1A–C), with an apparent decrease in levels between P14 and P30. Western blot analysis confirmed this developmental regulation (Fig. 1E). Immunolabelling and Western blot analysis reveal lack of FMRP expression in brain tissue from P10 *Fmr1* KO (Fig. 1D and E). Together, these findings are consistent with previous reports that FMRP is widely expressed in neurons throughout the mouse brain and that its expression level is dynamically regulated during postnatal development (13–15).

### Loss of FMRP is associated with subtle alterations in dendritic spines of pyramidal neurons

FXS has been characterized as a synaptopathy as defined by abnormalities in spine number, dynamics and morphology as well as dysregulated group 1 mGluR signalling (16), although associated spine density and morphology phenotypes are complex and depend on the age and cell-type being examined (17). To assess the consequences of deleting FMRP on dendritic spine density and morphology in rats, we quantified dendritic spines per unit length of dendrite from fluorescent-filled pyramidal neurons in the CA1 region of hippocampal slices (P27–P32) (Fig. 2A–C). Quantification of the number of dendritic protrusions revealed an increase in overall spine density on secondary apical obliques in *Fmr1* KO compared with WT (spines/10 µm WT:16.29 ± 0.55; KO:18.31 ± 0.68; $t_{14\_Welch\_cor} = 2.31$, $P = 0.037$). In contrast, spine density on secondary basal dendrites was comparable between genotypes (spines/10 µm WT:15.34 ± 0.70; KO:15.31 ± 0.79; $t_{14\_Welch\_cor} = 0.026$, $P = 0.98$).

Cumulative distributions of spine head diameter suggested a small, but significant increase in *Fmr1* KO compared with WT in both apical ($n_{WT} = 1218$, $n_{KO} = 1596$; $P = 0.0053$; Fig. 2D) and basal ($n_{WT} = 1106$, $n_{KO} = 1451$; $P = 0.0026$; Fig. 2E) CA1 secondary dendrites. These differences were not significant at the level of means [mean spine head diameter (MSHD) $WT_{apical}$:0.36 ± 0.0073 µm; $KO_{apical}$:0.38 ± 0.010 µm; $t_{14\_Welch\_cor} = 1.72$, $P = 0.11$, inset Fig. 2C; $WT_{basal}$:0.35 ± 0.011 µm, $n = 7$; $KO_{basal}$:0.36 ± 0.012 µm; $t_{14\_Welch\_cor} = 0.93$, $P = 0.37$, inset Fig. 2D]. These data are in agreement with recent findings in *Fmr1* KO mice using STED microscopy showing an increase in spine head width in CA1 pyramidal neurons at P37 (7).

### Abnormal synaptic plasticity in *Fmr1* KO rats

Group 1 mGluR-LTD in CA1 of the hippocampus is both exaggerated and independent of new protein synthesis in *Fmr1* KO mice (1,2). We therefore next asked whether loss of FMRP in rats alters the expression and/or maintenance of this form of plasticity in

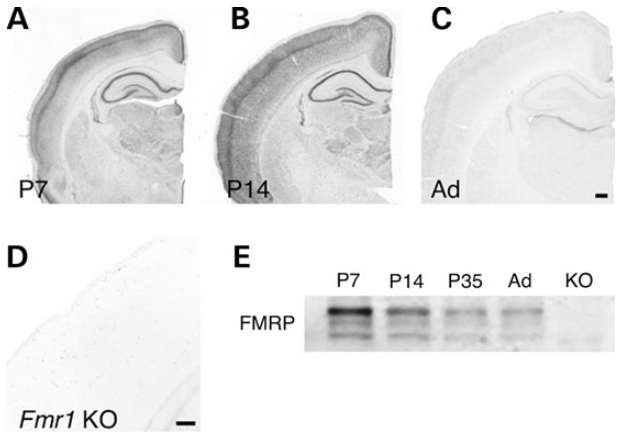


**Figure 1.** Developmental expression profile of FMRP in rats. Immunohistochemical localization of FMRP in P7 (**A**), P14 (**B**) and adult (**C**) WT SD rats. Immunolabelling of a P10 *Fmr1* KO shows specificity of antibody for FMRP (**D**). Western blot analysis of FMRP expression levels in hippocampus homogenates from WT SD rats littermates over postnatal development compared with P10 *Fmr1* KO rat (**E**). Scale bars: (A–C): 500 µm; (D) 250 µm.

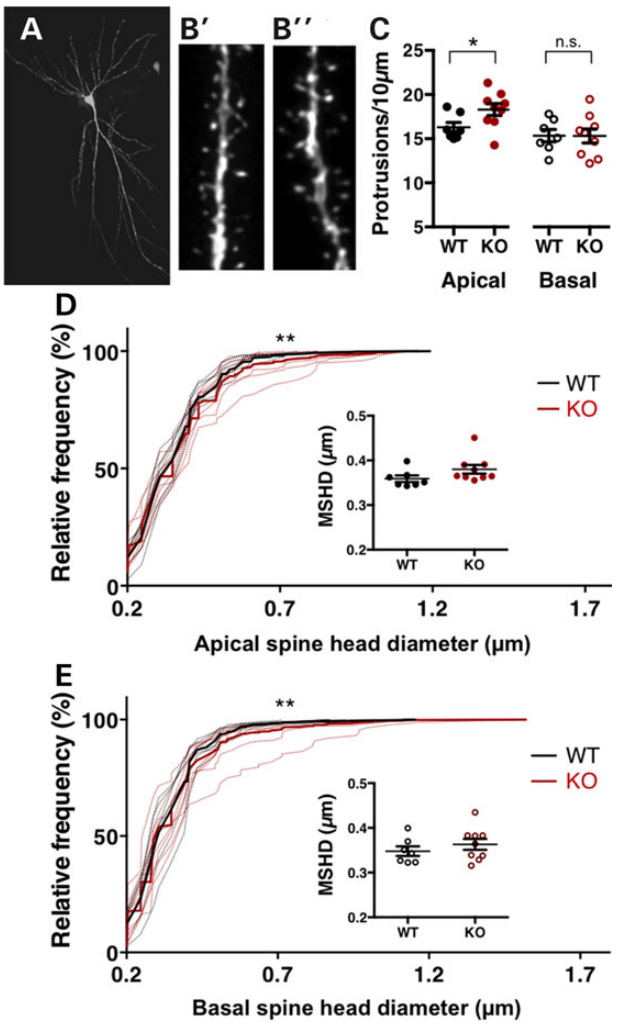


**Figure 2.** Altered dendritic spine density and shape in the hippocampus of *Fmr1* KO rats. An example Alexafluor 568 filled hippocampal CA1 pyramidal neuron (**A**) and representative apical oblique dendritic segments from WT (**B′**) and *Fmr1* KO rats (**B″**). (**C**) Quantification of the density of dendritic protrusions reveals a significant increase on secondary apical obliques in *Fmr1* KO rats compared with WT control littermates. In contrast, spine density of secondary basal dendrites is comparable between genotypes. KS-tests of the cumulative frequency distributions indicate differences in the distribution profiles of spine head diameters on apical (**D**) and basal (**E**) CA1 dendrites between *Fmr1* KO and WT rats. Dotted lines show the cumulative distribution for each animal, solid lines represent group means. The MSHD is not significantly different between genotypes.

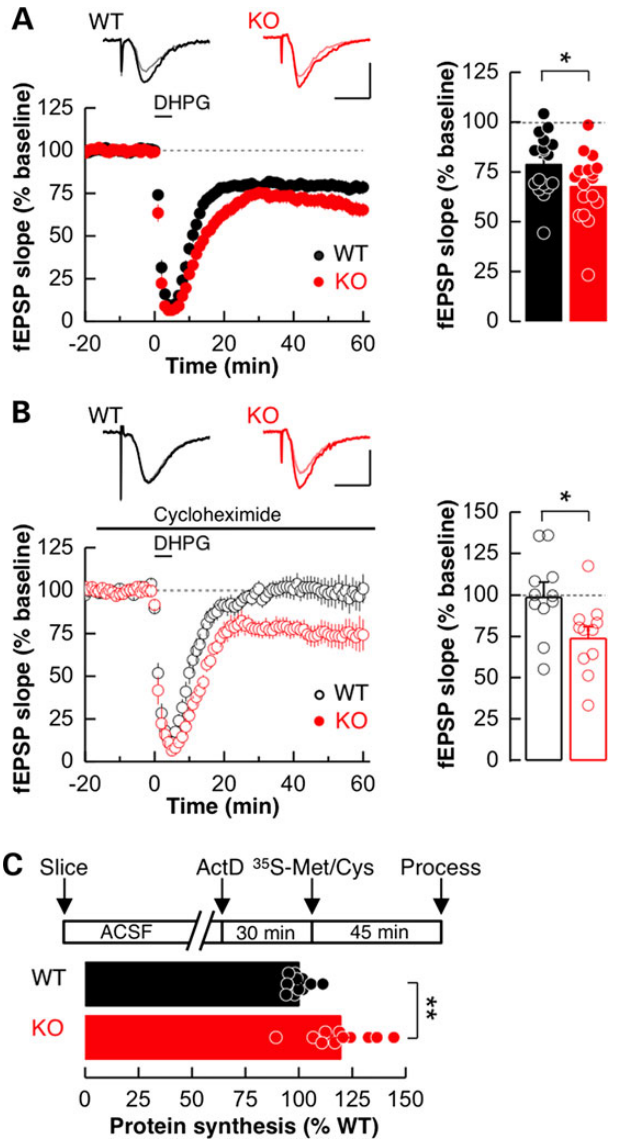


**Figure 3.** Loss of FMRP alters synaptic plasticity and basal protein synthesis in the rat hippocampus. (**A**) Sample fEPSP traces from 5 min pre- and 55 min post-DHPG treatment are shown above average fEPSP plots for both WT and *Fmr1* KO slices normalized to pre-DHPG baseline. (A) The magnitude of DHPG-induced LTD in WT and *Fmr1* KO rats was not significantly different between genotypes. (**B**) While the persistent expression of mGluR-LTD did not require new protein synthesis in *Fmr1* KO rats, mGluR-LTD was not maintained in WT rats in the presence of protein synthesis inhibitor cycloheximide. (**C**) Basal protein synthesis levels are excessive in dorsal hippocampal slices from *Fmr1* KO rats compared with WT littermate controls. Calibration bars for A and B: 0.5 mV, 10 ms.

the hippocampus. The magnitude of long-term depression (LTD) elicited by directly activating group I mGluRs with the agonist dihydroxyphenylglycine (DHPG) (1) was significantly greater in slices from *Fmr1* KO rats compared with control littermates (fEPSP responses WT:78.64 ± 3.70%, KO:67.53 ± 4.11%, $t_{32} = 2.0065$, $p_{WTvKO} = 0.027$; Fig. 3A). In addition, while the presence of the protein synthesis inhibitor cycloheximide prevented the maintenance of mGluR-LTD compared with baseline in WT animals, late-phase mGluR-LTD did not require new protein synthesis and was significantly different from baseline in *Fmr1* KO rats (fEPSP responses WT:98.08 ± 8.34%, KO:74.22 ± 7.42%, $t_{20} = 2.14$, $p_{WTvKO} = 0.023$; Fig. 3B).

Converging evidence suggests that FMRP negatively regulates the translation of its mRNA targets (3,18,19) and basal protein synthesis is elevated in *Fmr1* KO mice (4–6). Increased basal levels of proteins involved in persistent forms of plasticity may account for the protein synthesis-independent nature of mGluR-LTD in *Fmr1* KO mice. To test whether loss of FMRP in the rat results in increased basal protein synthesis, metabolic labelling of proteins in acute slices of dorsal hippocampus was compared between *Fmr1* KO and WT. Consistent with findings in *Fmr1* KO mice, loss of FMRP resulted in excessive protein synthesis under basal conditions (compared with baseline WT:100 ± 1.5%; KO:119.5 ± 4.6%; $t_{20} = 3.55$, $P = 0.0023$ Fig. 3C).

### Hippocampus-dependent behaviours in *Fmr1* KO rats

To begin to address whether cognitive function is altered by the loss of FMRP in rats, performance in a hippocampus-dependent reference memory version of the Morris water maze was tested. This task assays the ability to learn to navigate a circular pool using distal cues to locate a hidden, submerged escape platform. During acquisition, both WT and *Fmr1* KO rats showed a decrease in path length taken to reach the platform (training day $F_{(6,96)} = 21.894$, $P < 0.001$; genotype $F_{(1,16)} = 1.66$, $P = 0.22$; genotype × training day $F_{(6,96)} = 0.56$, $P = 0.76$; Fig. 4A), and increased crossings of the platform location during probe trials across days (training day $F_{(6,96)} = 4.112$, $P = 0.0010$; genotype $F_{(1,16)} = 3.666$, $P = 0.074$; genotype × training day $F_{(6,96)} = 1.41$, $P = 0.22$; Fig. 4B), indicating that spatial learning and memory was equivalent between genotypes and that *Fmr1* KO rats have intact capacity for spatial navigation. To assess behavioural flexibility, rats then underwent a reversal learning task whereby the platform was moved to the opposite side of the pool; a decrease in overall path length (training day $F_{(6,96)} = 27.585$, $P < 0.001$; genotype $F_{(1,16)} = 0.476$, $P = 0.50$; genotype × training day $F_{(6,96)} = 1.68$, $P = 0.13$; Fig. 4C), increase in crossings of the new platform location (training day $F_{new(6,96)} = 3.46$, $P = 0.0038$; genotype $F_{new(1,16)} = 0.30$, $P = 0.59$; genotype × training $F_{new(6,96)} = 1.18$, $P = 0.32$) and a concomitant decrease in crossings of the initial platform location during probe trials were observed across time (training day $F_{old(6,96)} = 12.322$, $P < 0.001$; genotype $F_{old(1,16)} = 3.21$, $P = 0.092$; genotype × training day $F_{new(6,96)} = 1.51$, $P = 0.18$; Fig. 4D), reflecting comparable learning of the second platform position between genotypes. While analysis of non-cognitive parameters revealed no difference in learning on the cued version of the task or in thigmotaxis (data not shown), swimming speed was significantly increased in *Fmr1* KO (genotype $F_{(1,16)} = 6.28$, $P = 0.023$; training day $F_{(13,208)} = 3.37$, $P < 0.001$; genotype × training day $F_{(13,208)} = 0.79$, $P = 0.67$; Fig. 4E).

To explore further whether loss of FMRP affects behavioural flexibility, we next used a DMP that is similar to the reference memory version of water maze except that the location of the platform is altered each day (Fig. 5A). This task assesses the ability of an animal to learn a novel location of a hidden platform in a single trial as measured by its performance in subsequent trials; a reduction in path length between the first and second trials of each day reflects the 'savings' accrued from the memory of the first trial. During pre-training, both WT and *Fmr1* KO rats showed decreases in path lengths taken to escape over trials 2–4 compared with the first trial of the day (trial $F_{D1\text{-}4(3,22)} = 21.19$, $P < 0.0001$; genotype $F_{D1\text{-}4(1,22)} = 0.21$, $P = 0.65$; genotype × trial $F_{D1\text{-}4(3,66)} = 0.86$, $P = 0.47$. trial $F_{D5\text{-}8(3,22)} = 19.10$, $P < 0.0001$; genotype $F_{D5\text{-}8(1,22)} = 0.23$, $P = 0.64$; genotype × trial $F_{D5\text{-}8(3,66)} = 0.18$, $P = 0.91$ Fig. 5B). In a second phase, the task was made more demanding by introducing variable time delays between the first and second trials of the day [15 s, 15 min or 2 h inter-trial intervals (ITI)]. During this phase, both WT and *Fmr1* KO performances were comparable at each ITI as measured by either the path lengths to escape (trial $F_{15sec(3,94)} = 1.55$, $P < 0.001$; genotype $F_{15sec(1,94)} = 0.85$, $P = 0.3586$; trial × genotype $F_{15sec(3,282)} = 1.553$, $P = 0.201$. trial

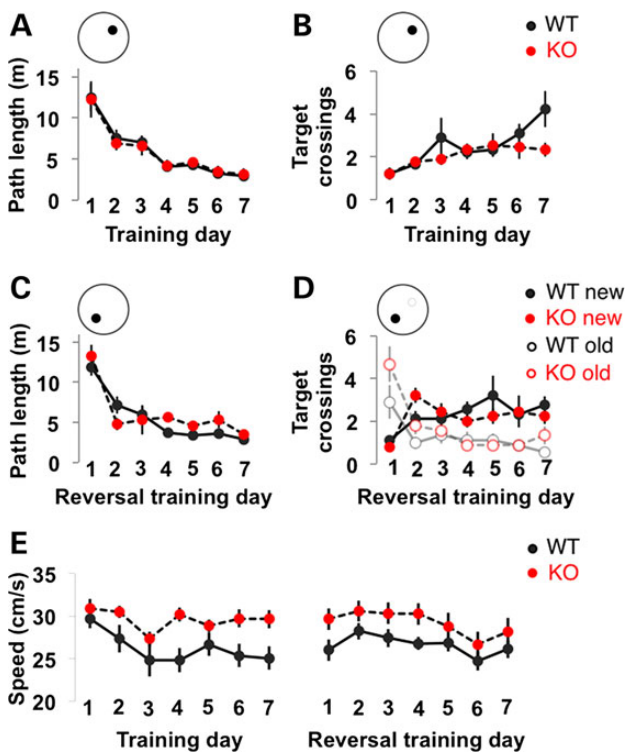


**Figure 4.** *Fmr1* KO rats have normal spatial reference memory acquisition and reversal learning. (**A**) *Fmr1* KO rats learn the hidden-platform version of the water maze similarly to WT littermates as measured by a decrease over days in the path taken to escape (A) and the number of crossings over the platform location on daily probe trials (**B**). Performance during reversal learning was comparable between genotypes as measured by path to escape (**C**) and the number of crossings over the old and new platform locations during probe trials (**D**). (**E**) *Fmr1* KO rats swim faster than WT littermates over all days tested.

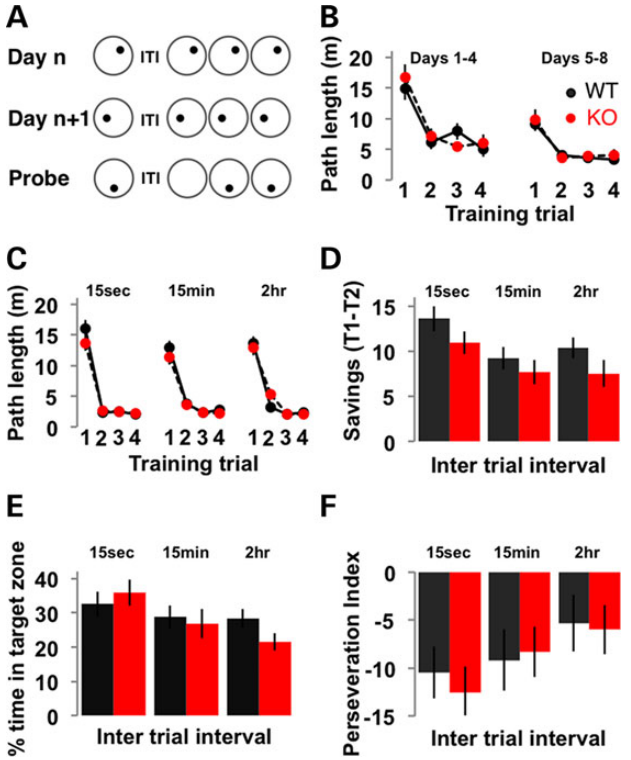


**Figure 5.** One-trial spatial learning is intact in *Fmr1* KO rats. (**A**) A schematic of the DMP version of the water maze task. (**B**) *Fmr1* KO rats learn the DMP task similarly to WT littermates as measured by a decrease in the path length taken to escape over trials within a day. Introducing a variable time delay between the first and second trials of the day does not affect performance of *Fmr1* KO rats compared with WT as measured by path length to escape (**C**), savings (**D**), time spent searching in the target zone on probe trials (**E**) or perseveration around the location of the target on the previous day on probe trials (**F**).

$F_{15min(3,94)} = 91.76$, $P < 0.001$; genotype $F_{15min(1,94)} = 1.68$, $P = 0.1986$; trial × genotype $F_{15min(3,282)} = 0.5612$, $P = 0.6411$. trial $F_{2hr(3,94)} = 113.5$, $P < 0.001$; genotype $F_{2hr(1,94)} = 0.21$, $P = 0.6481$; trial × genotype $F_{2hr(3,282)} = 1.63$, $P = 0.1824$; Fig. 5C) or by the savings accrued from trials one to two (delay $F_{(2,22)} = 4.77$, $P = 0.013$; genotype $F_{(1,22)} = 2.58$, $P = 0.1226$; delay × genotype $F_{(2,44)} = 0.14$, $P = 0.87$; Fig. 5D). Probe trials measuring time spent searching in the target zone further confirmed comparable one-trial spatial learning between genotypes across the ITIs (delay $F_{(2,22)} = 4.27$, $P = 0.0202$; genotype $F_{(1,22)} = 0.34$, $P = 0.5635$; delay × genotype $F_{(2,44)} = 1.26$, $P = 0.2942$; Fig. 5E) and comparison of the time spent in the location of the target on the previous day suggests no difference in perseveration between genotypes (delay $F_{(2,22)} = 2.07$, $P = 0.14$; genotype $F_{(1,22)} = 0.61$, $P = 0.44$; delay × genotype $F_{(2,44)} = 0.54$, $P = 0.59$; Fig. 5F).

To investigate further the effect of loss of FMRP on cognitive function, rats were tested on a battery of four spontaneous recognition memory tasks testing memory for object-recognition (OR) and object-context (OC), object-place (OP) and object-place-context (OPC) associations (Fig. 6A). Only, the most complicated of these, the OPC task, is hippocampus-dependent and involves the associative recognition of objects, their spatial locations and the local context (20). WT rats discriminated novel from familiar objects/object configurations in all four versions of the spontaneous exploration tasks, indicated by a discrimination index (DI) significantly greater than zero ($WT_{OR}$: 0.37 ± 0.03, $t_{15} = 11.26$, $P = 4.087 \times 10^{-8}$; $WT_{OP}$: 0.28 ± 0.056, $t_{15} = 5.031$, $P = 0.0006$; $WT_{OC}$: 0.28 ± 0.032, $t_{15} = 8.88$, $P = 9.34 \times 10^{-7}$; $WT_{OPC}$: 0.22 ± 0.041, $t_{15} = 5.32$, $P = 0.00035$; Fig. 6B). While *Fmr1* KO rats exhibited a significant preference for the novel object/object configurations in the OR, OC and OP tasks ($KO_{OR}$: 0.42 ± 0.038, $t_{15} = 11.20$, $P = 4.42 \times 10^{-8}$; $KO_{OP}$: 0.21 ± 0.051, $t_{15} = 4.112$, $P = 0.0037$; $KO_{OC}$: 0.18 ± 0.038, $t_{15} = 4.93$, $P = 0.00073$), they did not explore the novel OPC configuration more than expected by chance (DI $KO_{OPC}$: 0.071 ± 0.032, $t_{15} = 2.214$, $P = 0.17$; Fig. 6C). This suggests the impairment shown by *Fmr1* KO in OPC performance is not due to impairments in the associative recognition of objects and their locations or objects and their contexts.

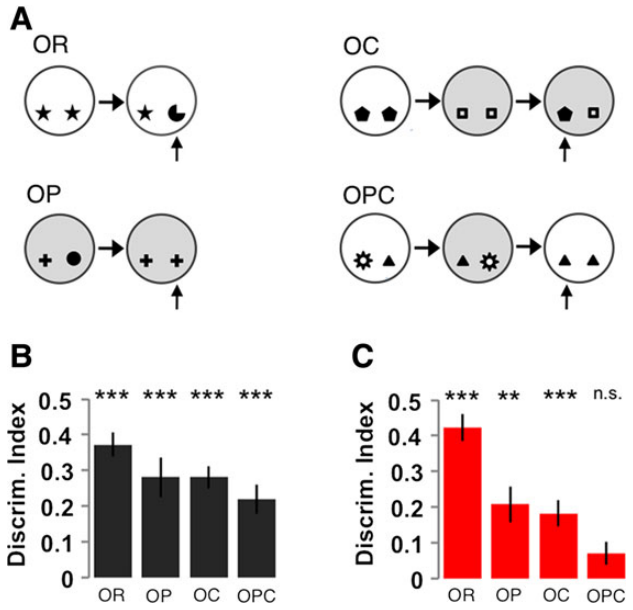


**Figure 6.** Loss of FMRP results in impaired performance on a hippocampus-dependent novelty preference task. (**A**) A schematic of the spontaneous exploration tasks for novelty preference. (**B**) WT rats exhibit memory for all four tasks as measured by above chance performance. (**C**) In contrast, *Fmr1* KO rats do not perform above chance levels in an OPC task that requires the ability to form associations between objects, their locations and the context, but do exhibit memory for the individual components as measured by above chance performance in object recognition, object-place and object-context tasks.

## Discussion

The development of genetically modified rat models provides a valuable means of understanding the cognitive dysfunction associated with the loss of FMRP, as well as providing cross-species validation of cellular dysfunction that will strengthen the relevance of genetic models of FXS to the human disorder. We find that *Fmr1* KO rats phenocopy key aspects of hippocampal cellular and synaptic phenotypes associated with the loss of FMRP in mice, including elevated basal protein synthesis (5), abnormal synaptic plasticity (1,2) and alterations in the morphology of dendritic spines (7) of hippocampal pyramidal neurons. Importantly, these phenotypes are commonly used to assess therapeutic efficacy for pharmacological reversal of FXS-related symptoms. As such, this study demonstrates cross-species validity of multiple cellular phenotypes associated with loss of FMRP between two mammalian species that separated in evolution more than 12 million years ago (12). It thereby validates the conceptual basis of theories underlying targeted approaches to therapies and their potential relevance to the human syndrome. It will be important in future studies to determine whether pharmaceutical interventions, such as negative allosteric modulators of mGluR5, are able to prevent or reverse these cellular deficits as they can in mice (5,21).

We also identified species-specific differences in cellular phenotypes between *Fmr1* KO models. For example, we find an increase in dendritic spine density on apical CA1 dendrites, a result which supports some (22,23), but not all studies in *Fmr1* KO mice (24). Importantly, differences in spine density are cell-type and age-dependent. In this study we have examined dendritic spine density at P28–P32 and found a small (12.4%) but significant increase in spine density on apical dendrites but no difference in basal dendritic spine density. Using STED microscopy we found no change in spine density at a similar age (P37) in mice (7). These apparent species differences could result from differences in methodologies; while STED is excellent for spine shape, the sample size is markedly smaller than confocal imaging for measurements of spine density. Furthermore, the biological significance of an increase in spine density of this magnitude is not known and more detailed studies relating spine structure to function are needed.

Species-specific differences were also apparent when we examined whether the common cellular phenotypes in the hippocampus in *Fmr1* KO mice and rats are mirrored by hippocampus-dependent behavioural phenotypes in the *Fmr1* KO rat. Despite *Fmr1* KO mice showing deficits in reversal learning in the water maze (8–11), this form of spatial learning is not affected by the loss of FMRP in rats. One-trial spatial learning in a hippocampus-dependent DMP water maze task was also unaffected in *Fmr1* KO rats. While this form of learning has not been tested in *Fmr1* KO mice, these findings are consistent with intact flexible spatial learning in *Fmr1* KO rats. These differences highlight the fact that common cellular dysfunction across species may manifest in distinct behavioural phenotypes and may result from species-specific differences associated with ethologically relevant tasks (25).

Importantly, while spatial learning was unaffected in *Fmr1* KO, we found significant deficits in hippocampus-dependent

associative recognition memory, but not in versions of these tasks that do not require an intact hippocampus. Complete hippocampal lesions impair performance on the OPC recognition task but do not alter performance on OR, OP and OC (20). We find that *Fmr1* KO rats are able to perform the OR, OP and OC tasks, but not the OPC recognition task that requires the hippocampus to bind multiple associations to form a memory. These data suggest that the loss of FMRP selectively affects a subset of hippocampus-dependent processes that include memory/binding of complex associations. Understanding how these differences arise will require a detailed analysis of the mechanisms by which cellular dysfunction affects neuronal circuit activity to ultimately control behaviour.

In summary, this study reveals valuable insight into the defects in episodic-like memory associated with the loss of FMRP. Furthermore, by demonstrating that the cellular pathophysiology associated with the loss of FMRP is shared between mice and rats, our study provides the foundation for interpretation of subsequent investigations of hippocampal function that utilises the biological and technical advantages afforded by rat models. For example, future studies can take advantage of their increased flexibility in response to novel situations and their extensive social interactions—two domains specifically affected in FXS and the autism spectrum disorders. In this context, deficits in perseverative chewing and juvenile play have been reported in *Fmr1* KO rats (26). Furthermore, they can include the use of fMRI/PET scanning that will enable the identification of circuit level biomarkers that can be useful for translation into humans as well as drug screening and clinical trial design. As a result, rat-based disease models will complement existing mouse models and together they may provide new insight into mechanisms and behavioural outcomes of FMRP dysregulation in humans.

## Materials and Methods

### Animals

SD *Fmr1* KO rats were obtained from Sigma Advanced Genetic Engineering (SAGE) Labs (St. Louis, MO, USA), now part of Horizon Discovery. Female *Fmr1* heterozygotes were crossed to WT SD males (Charles River labs) to produce *Fmr1* KO and WT littermate controls. All experimental subjects were male and group housed (2–5 animals/cage) to avoid effects of isolation. Experiments were done blind to genotype.

### Immunoblotting

Hippocampal extracts from *Fmr1* KO rats and controls ($n = 3$/age for developmental expression; $n = 5$/genotype at P10 to verify loss of expression) were prepared in RIPA buffer containing protease inhibitors (Complete EDTA-free), immunoblotted using primary antibody to FMRP (1:2000; AbCAM ab69815) and imaged as previously described in (13).

### Immunohistochemistry

Histology was performed as previously described (13). Coronal sections were reacted with an antibody to FMRP (1:1500, Millipore MAB2160).

### Basal protein synthesis

Metabolic labelling of transverse slices prepared from P28 rats ($n = 11$/genotype) was performed as described (6).

### Intracellular fills and analysis

Individual hippocampal CA1 pyramidal neurons from P27 to P32 males ($n_{WT} = 7$, $n_{KO} = 9$) were filled with Alexafluor-568, imaged, deconvolved and spine densities quantified as in Till *et al.* (2012). Dendritic spine head diameters were measured using the 'shortest distance from distance map' algorithm (IMARIS FilamentTracer, Bitplane); spines with an obvious point of attachment to the dendritic shaft were quantified. Head diameters <200 nm were excluded from analysis, due to the resolution of the confocal microscope.

### Electrophysiology

Horizontal hippocampal slices (400 µm) prepared from P21 to P32 animals were incubated in oxygenated ACSF at 31°C for 30 min, then stored at room temperature until recording. An incision was made through CA3 prior to recording. Slices were continuously perfused in an interface chamber with 30 ± 1°C ACSF saturated with 95% $O_2$-5% $CO_2$ at 4–5 ml/min. Field potentials were recorded as described in Huber *et al.* (2002). mGluR-LTD was induced using dihydroxyphenylglycine (DHPG; 50 µM) in the presence of NMDA receptor antagonist D-AP5 (50 µM) for 5 min. Where indicated, cycloheximide (100 µM) was present in ACSF >30 min prior to DHPG addition and throughout recordings. LTD magnitude was calculated by dividing the average fEPSP slope from 50 to 60 min post-DHPG application by the average fEPSP slope during the 20 min baseline before DHPG application.

### Spatial reference memory water maze

Three- to six-month old male rats ($n_{WT} = 9$, $n_{KO} = 9$) were trained in three stages in a 2 m diameter water maze containing a 10 cm escape platform. First, rats were trained for 3 days on the visible platform version of the water maze (4 trials/day, 15 min ITI, extra-maze cues obscured, platform location moved each trial). In the second stage, extra-maze cues were visible and rats received one daily hidden-platform training session for seven consecutive days; each session began with a reinforced probe trial, followed by three training trials separated by a 15 min ITI. For probe trials, an Atlantis platform (27) was raised to 1.5 cm below the water surface 1 min into the trial; for standard trials the platform was raised throughout. Each trial lasted a maximum of 2 min; rats failing to escape were guided to the platform. All rats remained on the platform for 30 s before removal from the pool. The third (reversal) stage was identical to the second, but the platform was relocated to the opposite side of the pool. Path length performance is plotted in meters (m) was compared to account for differences in swim speed. For probe trials, target crossings during the first 60 s were quantified.

### DMP water maze

Three- to six-month old male rats ($n_{WT} = 12$, $n_{KO} = 12$) were trained on a modified version of a DMP task in the water maze (28). The protocol for both pre-training and delay phases were the same; the platform was hidden in a novel location on trial 1 of each day and then remained in this place for trials 2–4, on which rats could use rapidly encoded place memory to reach the escape platform efficiently. The different platform locations were located on an inner ring (0.8-m diameter) or outer ring (1.4 m) concentric with the pool. Each trial lasted a maximum of 2 min; rats failing to escape were guided to the platform. All rats remained on the platform for 30 s before removal from the pool. All four start positions were used daily in an arbitrary sequence, to discourage egocentric strategies. During the first phase, rats received two 4-day

blocks of pre-training (4 trials/day, 15 s ITI, extra-maze cues visible, platform location moved each day). In the second phase, rats received 15 days of delay training during which three different ITIs (15 s, 15 min or 2 h) were introduced between trials 1 and 2 (5 days of each ITI); for one of the 5 days at each delay, trial 2 of the day was run as a probe trial with an Atlantis platform (27) raised to 1.5 cm below the water surface 1 min into the trial; for standard trials the platform was raised throughout. Probe trial performance was calculated as the percent time spent in a 20 cm diameter zone around the centre of the platform location during the first 60 s. Perseveration index indicates the difference between the percent time spent in the previous day's target zone and the current day's target zone during the first 60 s of the probe trial.

### Spontaneous exploration tasks

Three- to six-month old male rats ($n_{WT} = 16$, $n_{KO} = 16$) underwent OR, OP, OC and OPC tasks as previously described (20). Animals were tested in a rectangular box (76 × 45 × 60 cm tall) that could be configured as either of two contexts (by changing floor/wall inserts). After 5 days habituation to the boxes, rats received 2 trials (one/day) on each of the four tasks (OR, OP, OC, OPC, OPC, OC, OP, OR), with 3 min sample phases, a 2 min retention interval and a 3 min test phase. For each test phase, a DI [(time exploring novel object—time exploring familiar object)/(time exploring both objects)] was calculated.

### Statistical analysis

Electrophysiology data were analysed using one-tailed Student's *t*-test. Dendritic spine density data were analysed by unpaired *t*-test with Welch's correction. Dendritic head diameter measures were analysed with two-sample Kolmogorov–Smirnov test (KS-test) and Mann–Whitney test (MW-test). Water maze data were analysed by repeated measures ANOVA and spontaneous exploration task discrimination indices were analysed by one sample *t*-test (chance = 0) with Bonferroni correction. Except in the case of dendritic spine head measures, the independent replicate (*n*) is experimental animals. Error bars in graphs represent ± SEM; $^{*}P < 0.05$, $^{**}P < 0.01$, $^{***}P < 0.001$.

## Acknowledgements

This work was supported by funds from the Medical Research Council (G0700967, MR/K014137/1 to P.C.K. and D.J.A.W., the Department of Biotechnology, India to S.C., P.C.K.), Wadhwani Foundation (S.C.), The Shirley Foundation (P.C.K.), The Patrick Wild Centre (P.C.K., S.M.T., E.R.W.), the RS MacDonald Trust (P.C.K., S.M.T.), the Wellcome Trust-University of Edinburgh Institutional Strategic Support Fund (P.C.K., S.M.T.), Scottish University Life Sciences Alliance (P.C.K., S.M.T.), Autistica (S.M.T.) and Greek State Scholarship Foundation (IKY), Maria Zausi bequest (A.A.). We thank our colleagues for constructive discussions during the course of this study and Trudi Gillespie from the IMPACT imaging facility at the University of Edinburgh for help with microscopy.

*Conflict of Interest statement*. M.F.B. holds patents on the use of mGluR5 inhibitors for the treatment of fragile X.

## Funding

This work was supported by funds from the Medical Research Council (G0700967, MR/K014137/1 to P.C.K. and D.J.A.W., the Department of Biotechnology, India to S.C., P.C.K.), Wadhwani Foundation (S.C.), The Shirley Foundation (P.C.K.), The Patrick Wild Centre (P.C.K., S.M.T., E.R.W.), the RS MacDonald Trust (P.C.K., S.M.T.), theWellcome Trust-University of Edinburgh Institutional Strategic Support Fund (P.C.K., S.M.T.), Scottish University Life Sciences Alliance (P.C.K., S.M.T.), Autistica (S.M.T.) and Greek State Scholarship Foundation (IKY), Maria Zausi bequest (A.A.). Funding to pay the Open Access publication charges for this article was provided by RCUK Open Access Fund.

## References

1. Huber, K.M., Gallagher, S.M., Warren, S.T. and Bear, M.F. (2002) Altered synaptic plasticity in a mouse model of fragile X mental retardation. *Proc. Natl. Acad. Sci. U S A*, **99**, 7746–7750.
2. Nosyreva, E.D. and Huber, K.M. (2006) Metabotropic receptor-dependent long-term depression persists in the absence of protein synthesis in the mouse model of Fragile X Syndrome. *J. Neurophysiol.*, **95**, 3291–3295.
3. Darnell, J.C. and Klann, E. (2013) The translation of translational control by FMRP: therapeutic targets for FXS. *Nat. Neurosci.*, **16**, 1530–1536.
4. Qin, M., Kang, J., Burlin, T.V., Jiang, C. and Smith, C.B. (2005) Postadolescent changes in regional cerebral protein synthesis: an in vivo study in the FMR1 null mouse. *J. Neurosci.*, **25**, 5087–5095.
5. Dolen, G., Osterweil, E., Rao, B.S., Smith, G.B., Auerbach, B.D., Chattarji, S. and Bear, M.F. (2007) Correction of fragile X syndrome in mice. *Neuron*, **56**, 955–962.
6. Osterweil, E.K., Krueger, D.D., Reinhold, K. and Bear, M.F. (2010) Hypersensitivity to mGluR5 and ERK1/2 leads to excessive protein synthesis in the hippocampus of a mouse model of fragile X syndrome. *J. Neurosci.*, **30**, 15616–15627.
7. Wijetunge, L.S., Angibaud, J., Frick, A., Kind, P.C. and Nagerl, U.V. (2014) Stimulated emission depletion (STED) microscopy reveals nanoscale defects in the developmental trajectory of dendritic spine morphogenesis in a mouse model of fragile X syndrome. *J. Neurosci.*, **34**, 6405–6412.
8. Baker, K.B., Wray, S.P., Ritter, R., Mason, S., Lanthorn, T.H. and Savelieva, K.V. (2010) Male and female Fmr1 knockout mice on C57 albino background exhibit spatial learning and memory impairments. *Genes Brain Behav.*, **9**, 562–574.
9. Van Dam, D., D'Hooge, R., Hauben, E., Reyniers, E., Gantois, I., Bakker, C.E., Oostra, B.A., Kooy, R.F. and De Deyn, P.P. (2000) Spatial learning, contextual fear conditioning and conditioned emotional response in Fmr1 knockout mice. *Behav. Brain Res.*, **117**, 127–136.
10. Paradee, W., Melikian, H.E., Rasmussen, D.L., Kenneson, A., Conn, P.J. and Warren, S.T. (1999) Fragile X mouse: strain effects of knockout phenotype and evidence suggesting deficient amygdala function. *Neuroscience*, **94**, 185–192.
11. D'Hooge, R., Nagels, G., Franck, F., Bakker, C.E., Reyniers, E., Storm, K., Kooy, R.F., Oostra, B.A., Willems, P.J. and De Deyn, P.P. (1997) Mildly impaired water maze performance in male Fmr1 knockout mice. *Neuroscience*, **76**, 367–376.
12. Gibbs, R.A., Weinstock, G.M., Metzker, M.L., Muzny, D.M., Sodergren, E.J., Scherer, S., Scott, G., Steffen, D., Worley, K.C., Burch, P.E. *et al.* (2004) Genome sequence of the Brown Norway rat yields insights into mammalian evolution. *Nature*, **428**, 493–521.
13. Till, S.M., Wijetunge, L.S., Seidel, V.G., Harlow, E., Wright, A.K., Bagni, C., Contractor, A., Gillingwater, T.H. and Kind, P.C. (2012) Altered maturation of the primary somatosensory cortex in a mouse model of fragile X syndrome. *Hum. Mol. Genet.*, **21**, 2143–2156.

14. Irwin, S.A., Swain, R.A., Christmon, C.A., Chakravarti, A., Weiler, I.J. and Greenough, W.T. (2000) Evidence for altered Fragile-X mental retardation protein expression in response to behavioral stimulation. *Neurobiol. Learn. Mem.*, **74**, 87–93.
15. Christie, S.B., Akins, M.R., Schwob, J.E. and Fallon, J.R. (2009) The FXG: a presynaptic fragile X granule expressed in a subset of developing brain circuits. *J. Neurosci.*, **29**, 1514–1524.
16. Portera-Cailliau, C. (2012) Which comes first in fragile X syndrome, dendritic spine dysgenesis or defects in circuit plasticity? *Neuroscientist*, **18**, 28–44.
17. Wijetunge, L.S., Chattarji, S., Wyllie, D.J. and Kind, P.C. (2013) Fragile X syndrome: from targets to treatments. *Neuropharmacology*, **68**, 83–96.
18. Laggerbauer, B., Ostareck, D., Keidel, E.M., Ostareck-Lederer, A. and Fischer, U. (2001) Evidence that fragile X mental retardation protein is a negative regulator of translation. *Hum. Mol. Genet.*, **10**, 329–338.
19. Li, Z., Zhang, Y., Ku, L., Wilkinson, K.D., Warren, S.T. and Feng, Y. (2001) The fragile X mental retardation protein inhibits translation via interacting with mRNA. *Nucleic Acids Res.*, **29**, 2276–2283.
20. Langston, R.F. and Wood, E.R. (2010) Associative recognition and the hippocampus: differential effects of hippocampal lesions on object-place, object-context and object-place-context memory. *Hippocampus*, **20**, 1139–1153.
21. Michalon, A., Sidorov, M., Ballard, T.M., Ozmen, L., Spooren, W., Wettstein, J.G., Jaeschke, G., Bear, M.F. and Lindemann, L. (2012) Chronic pharmacological mGlu5 inhibition corrects fragile X in adult mice. *Neuron*, **74**, 49–56.
22. Bhattacharya, A., Kaphzan, H., Alvarez-Dieppa, A.C., Murphy, J.P., Pierre, P. and Klann, E. (2012) Genetic removal of p70 S6 kinase 1 corrects molecular, synaptic, and behavioral phenotypes in fragile X syndrome mice. *Neuron*, **76**, 325–337.
23. Gross, C., Chang, C.W., Kelly, S.M., Bhattacharya, A., McBride, S.M., Danielson, S.W., Jiang, M.Q., Chan, C.B., Ye, K., Gibson, J.R. *et al.* (2015) Increased expression of the PI3 K enhancer PIKE mediates deficits in synaptic plasticity and behavior in fragile X syndrome. *Cell Reports*, **11**, 727–736.
24. He, C.X. and Portera-Cailliau, C. (2013) The trouble with spines in fragile X syndrome: density, maturity and plasticity. *Neuroscience*, **251**, 120–128.
25. Gerlai, R. and Clayton, N.S. (1999) Analysing hippocampal function in transgenic mice: an ethological perspective. *Trends Neurosci.*, **22**, 47–51.
26. Hamilton, S.M., Green, J.R., Veeraragavan, S., Yuva, L., McCoy, A., Wu, Y., Warren, J., Little, L., Ji, D., Cui, X. *et al.* (2014) Fmr1 and Nlgn3 knockout rats: novel tools for investigating autism spectrum disorders. *Behavioral Neuroscience*, **128**, 103–109.
27. Spooner, R.I., Thomson, A., Hall, J., Morris, R.G. and Salter, S.H. (1994) The Atlantis platform: a new design and further developments of Buresova's on-demand platform for the water maze. *Learn. Mem.*, **1**, 203–211.
28. Steele, R.J. and Morris, R.G. (1999) Delay-dependent impairment of a matching-to-place task with chronic and intrahippocampal infusion of the NMDA-antagonist D-AP5. *Hippocampus*, **9**, 118–136.